Corona and Electric Field Distribution Analysis in 400 kV Line Insulators

Ragaleela Dalapati Rao[1,*], Padmanabha Raju Chinda[1], Meduri Kiran[2]

[1]Department of Electrical & Electronics Engineering, P.V.P Siddhartha Institute of Technology, Vijayawada, India

[2]Electrical Design Engineer, Leoni, Waterloo, Canada

Abstract

The performance of insulator strings in transmission lines can be improved by corona rings owing to their electric field grading property. The insulation performance of the string depends on the corona ring parameter settings. In this study, the design of a corona ring for a 400 kV non-ceramic overhead line insulator is presented. Two parameters were altered during the investigation, ring measurement (R) and ring tube breadth (r) while maintaining a constant ring height (h). Based on electric field distribution, the proposed composite insulators were compared with glass insulators. Simulation studies were performed for the insulator strings, including corona rings with different design parameters. The corona discharge and optimal configuration results were analyzed, and it was found that the electric field was lower with composite insulators.

1. Introduction

Insulators can be categorized into suspension and line post insulators [1]. Suspension insulators (such as porcelain and glass) are mainly used for stress stacking. However, generally non-ceramic insulators (NCIs) are used these days. NCI's are also called polymeric or composite insulators. Silicon rubber has good electrical properties and climate obstruction properties over a wide range of temperatures and is utilized in lodging. It is resistant to oxidation and deterioration from ultraviolet radiation and has low surface vitality. These properties settle on the silicon rubber and it can be effectively used for electrical insulators [2]. Previous studies have shown that the electric field distribution along composite insulators can be enhanced by incorporating various corona ring designs, which can also limit the corona ring related issues.

Extremely strong electric fields can offer ascent to a group of ionization in the encompassing air that comes full circle in the arrangement of corona releases [3]. One of the key procedures engaged with the inception and improvement of releases is the ionization of particles and atoms by high vitality electrons. Without any extremely applied electric field, the electrons move arbitrarily colliding with the gas atoms [4]. Within the sight of the electric field, be that as it may, the electrons are excited by the electric field and velocity toward the field [5]. The corona discharge occurs on the transmission-line conductors when the strength of the electric field on the conductor surface is greater than a specific value. This results in power loss, audible noise, production of gaseous effluents, and light [6]. In non-uniform fields, the self-sustained release is constrained within the air gap, and the corona discharge occurs as a result of the "partial breakdown". There are various modes of the corona discharge: alternating current (AC) corona and direct current (DC) corona. The underlying process of the AC corona discharge in every half cycle of the AC power frequency is fundamentally the same as those under DC voltages of the same polarity. Under AC

---

* Corresponding author. E-mail address: raga_233@yahoo.co.in

 Tel.: +91-9949418868

voltage, the corona initially shows up in the negative half cycle as Trichel streamers. As the voltage is increased, Trichel streamers begin to spark. In the following positive half cycle, the breakdown streamer follows the sparkle corona [7]. The positive corona discharge is a significant source of the radio interference voltage (RIV) and audible noise, and it causes deterioration of the rubber housing on the NCIs. Therefore, the corona should be avoided as much as possible while avoiding too much over-designed. Contingent upon the utilization and physical layout of a silicon insulator, a corona ring is generally introduced at the transmission line end to ensure line voltages of 230 kV. Nevertheless, the utilization of corona rings decreases the dry arcing separation of insulators. Therefore, it is important to structure the corona ring for the ideal review of the electric stress along the insulator.

This study investigates the electric field and potential distributions of glass and silicon rubber insulators. The results are obtained by utilizing the COMSOL Multi-physics software. The simulation results demonstrate that for the values acquired for the silicon rubber insulator with a corona ring (particularly for 220kV), the potential distribution along the insulator can be improved. Moreover, the electric stress can be decreased further for the insulator with the corona rings, compared with those of the insulators without corona rings and glass insulators [8]. To comprehensively understand the corona mechanisms and provide potential mitigation solutions, the corona onset and corona ring optimization are discussed in Section 2. The COMSOL modeling assumptions, related specifications, and the simulation results, including electric field, and potential distributions are provided in Section 3. The corona ring design is optimized based on 15 different ring sizes. The conclusion in Section 4 summarizes this study.

2. Corona Onset

The corona onset is defined as the occurrence of a self-sustained discharge. Townsend's law defines:

(1) The ionization coefficient α as the number of electron-particle sets formed in the gas by a single electron traveling through a unit distance separation toward the development of the electron.

(2) The attachment coefficient η as the likelihood that a free electron will join itself to an unbiased molecule to form a negative particle while moving through a unit distance separation through the gas toward the applied electric field.

Therefore, the equation can be expressed as

$$dn = n(x)(\alpha - \eta)dx \tag{1}$$

where α is the ionization coefficient and η is the attachment coefficient.

Integrating Eq. (1) on both sides:

$$\int \frac{dn}{n(x)} = \int_0^x (\alpha - \eta)dx \tag{2}$$

Therefore, Eq. (2) becomes:

$$n = n_0 e^{\int_0^x (\alpha - \eta)dx} \tag{3}$$

where n_0 is the number of electrons at $x=0$.

Now, if the electric field intensity is strong enough, the total number of electrons below approaches infinity (that is self-sustained discharge), thereby causing breakdown:

$$n = \frac{n_0}{1 - \gamma e^{\int_0^x (\alpha - \eta) dx}}$$
(4)

In other words, the breakdown occurs when

$$1 = \gamma e^{\int_0^x (\alpha - \eta) dx}$$
(5)

where γ is the secondary ionization coefficient in Eqs. (4) and (5) [6].

As defined above, the corona onset is characterized as the phenomenon of a self-sustained discharge. An observational equation was proposed in a previous study [9] based on smooth cylindrical conductors given in Eq. (6) [6]:

$$E_{gc} = m E_{0c} \delta [1 + \frac{C_a}{\sqrt{\delta r_c}}]$$
(6)

where

E_{gc} is the corona onset gradient in kV/mm

E_{0c} is an empirical constant of 2.11 kV- rms/mm

C_a is an empirical constant that Peek [9] determined to be 0.301 cm$^{-1/2}$

m is the conductor irregularity factor

δ is the relative air density, and

r_c is the radius of the conductor in meters

For the purpose of simulations in this study, a corona inception threshold of 2.2kV-rms/mm has been considered [10].

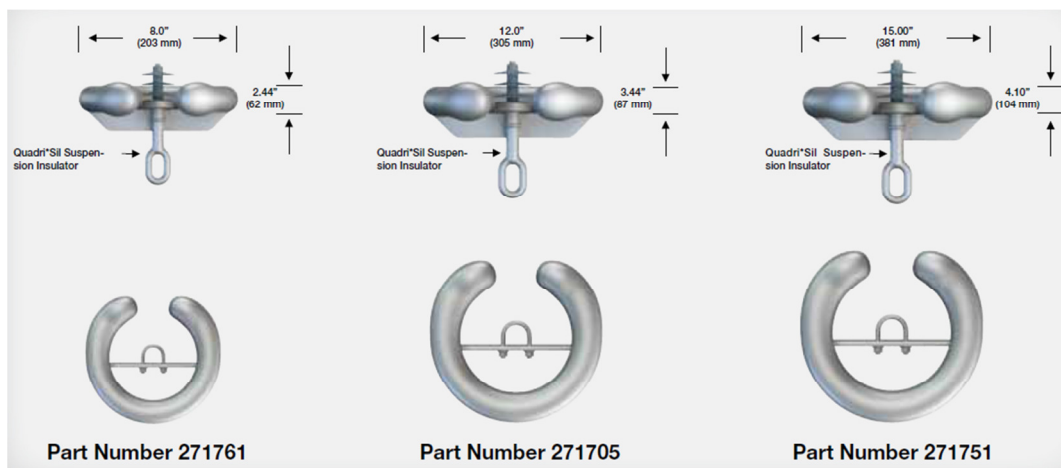### 2.1. Corona ring designs

Fig. 1 Corona ring sizes along with their part numbers [11]

As a result of all the negative corona effects, an attempt has been made to control the field distribution along the strings through the corona rings [12] and to protect the insulator string from direction power arcs [13]. Standard corona rings [14-15] (manufactured by Hubbell Power Systems Inc.) for transmission insulators are shown in Table 1 and Fig. 1 [11]. (where kip is Kilo pound and kN is Kilo newton).

Table 1 Standard transmission corona rings by Hubbell

Line Voltage (kV)	Recommended Corona Rings based on Line Voltage		Corona Ring Part Numbers			
	Ground End	Line End	25kip, 30kip, 120kN, 133kN		50kip, 160kN, 210kN	
			Ground End	Line End	Ground End	Line End
220/230	None	8 inches (203mm)	-	2717613001	-	2717613002
330/345	None	12 inches (305mm)	-	2717053001	-	2717053002
400	8 inches (203mm)	12 inches (305mm)	2717613001	2717053001	2717613002	2717053002
500	8 inches (203mm)	15 inches (381mm)	2717613001	2717513001	2717613002	2717513002

2.2. *Corona ring optimization*

As shown in Fig. 2 [10], the different specifications of corona rings are given below [16]:

(1) Ring measurement (R)

(2) Ring tube breadth (r)
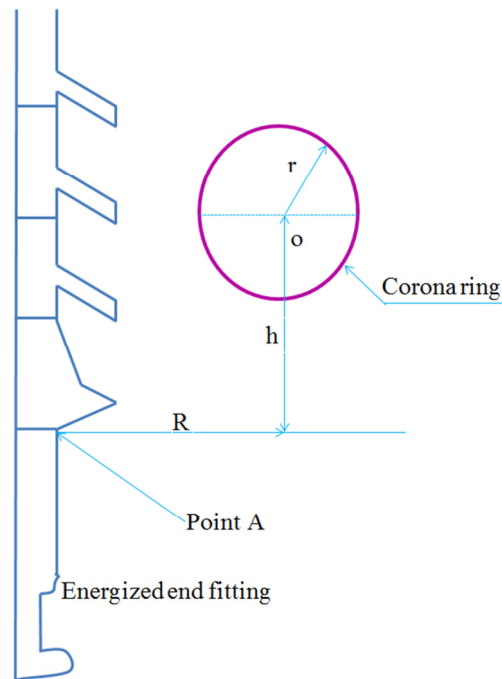
(3) Position of the ring in its vertical plane (h)
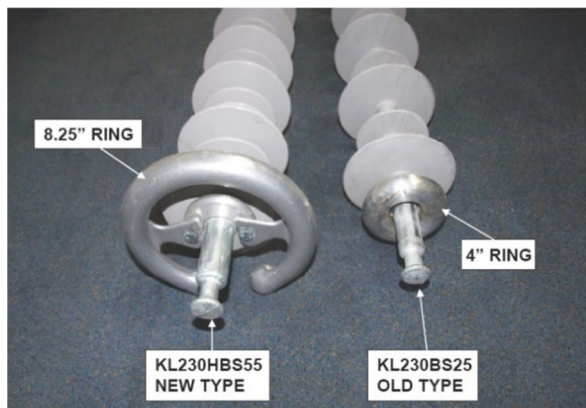

Fig. 2 Corona ring optimization specifications [17]
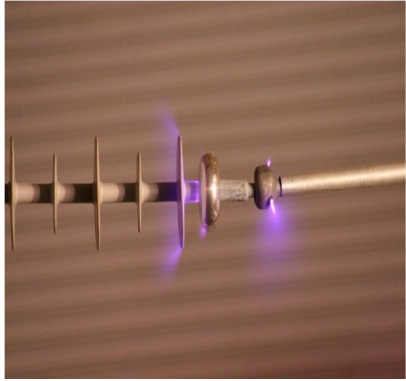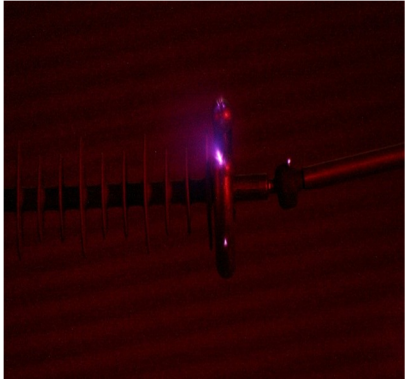

Fig. 3 New vs. old corona rings [18]

By changing any one or a combination of these specifications, the resulting electric field distribution can be modified [19-22]. In this study, it is assumed that h is a constant and the R and r values are optimized. Before the further discussion on

the simulation parameters and optimization, it is worthwhile to present a laboratory case study on a 133 kV dead-end line insulator. To demonstrate the effect of corona on small and large ring sizes, the ring sizes of 4 inches and 8.25 inches have been considered. Two different ring diameters have been considered as shown in Fig. 3 [7]. Table 2 illustrates that the smaller old design based ring (4 inches) clearly exhibits more corona activities compared with the new design based ring (8.25 inches) for 133kV and 146kV, as observed using a laboratory camera.

Table 2 Laboratory results comparing new and old design based corona rings

	With old corona ring (4 inches)	With new corona ring (8.25 inches)
133kV (100% voltage)		
146kV (110% voltage)		
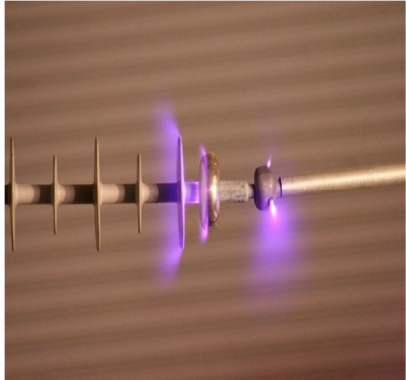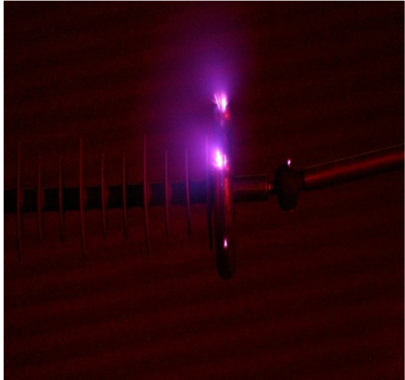
3. Results and Analysis

In this study, the overall analysis can be divided into two categories. One part of the analysis is based on the comparison between the glass and silicon suspension insulators to study the electric field distribution (part 1). The other part (part 2) of the analysis considers the silicon suspension insulators with corona ring optimization for 15 different ring sizes. The modeling assumptions of the suspension insulators are outlined in Table 3. The mesh settings [23] for both glass and silicon rubber insulators are shown in Figs. 4-6. The materials used for the simulations are listed in Table 4 [24-25]. The finite element analysis in COMSOL has been performed using stationary and frequency domain (60 Hz) solvers.

Table 3 Modeling assumptions of suspension insulators

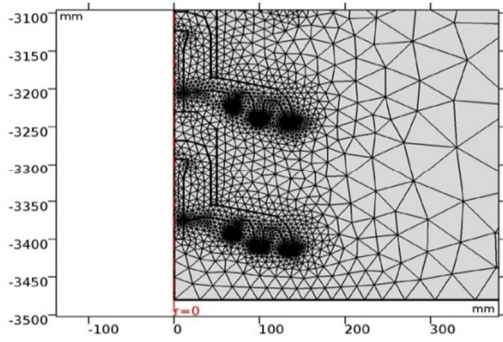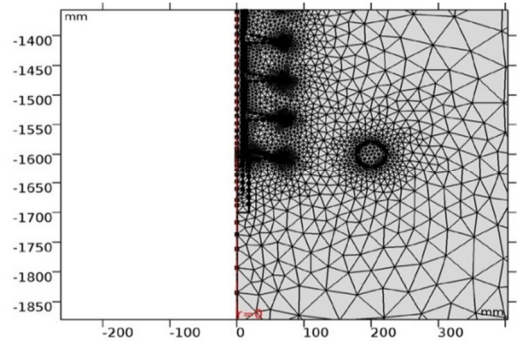| Insulator	Number	Length (mm)
Glass	20 (cap-and-pin)	3400
Silicon rubber	50 (identical silicon sheds)	1700

Fig. 4 Mesh settings

Fig. 5 Glass insulator meshing

Fig. 6 Silicon rubber insulators with corona ring meshing

Table 4 Materials used in simulations

Materials	Electrical Characteristics		
	Relative permeability (μ_r)	Electrical conductivity (σ)	Relative permittivity (ε_r)
Steel AISI 4340	1	4.032E6 S/m	1000
Silicon	1	1E-12 S/m	3
Glass (quartz)	1	1E-14 S/m	4.2
Air	1	0 S/m	1

3.1. Part 1

The electric field distribution and potential distribution of glass insulators for the different scenarios are shown in Figs. 7-8 (COMSOL screenshots). The electric field and potential distributions of silicon rubber insulators for the different scenarios are shown in Figs. 9-10. The 3-D plots of these insulators are shown in Figs. 11-12. The maximum electric field of the glass insulator on the line-end conductor is obtained at 14.83kV/mm corresponding to r = 11 mm and h = -3400 mm as shown in Fig. 7. Similarly, Fig. 9 shows the maximum electric field on the line-end conductor of the silicon rubber insulator, obtained at 3.03 kV/mm, corresponding to r = 18 mm and h = -1700 mm.

(a) Streamlines

(b) Overall
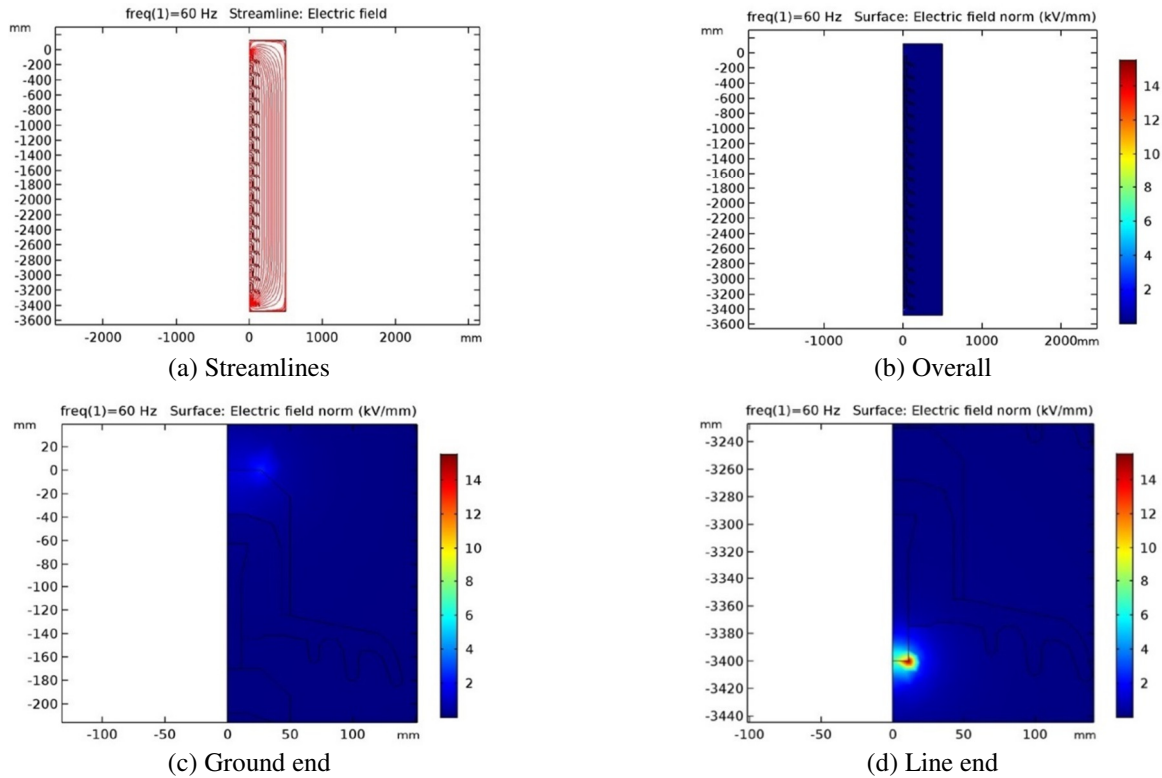

(c) Ground end

(d) Line end

Fig. 7 Electric field distribution of glass insulators for different scenarios

Therefore, from these figures, it is noted that silicon rubber insulators are prone to less stress (minimum electric field distribution) and the improvement of potential distribution along the insulator is contrasted with that of the glass insulators.

Because the maximum surface conductor electric field is higher than the corona inception threshold of 2.2 kV/mm in the silicon rubber insulator, the corona discharge will be observed. Accordingly, the application of corona rings to silicon rubber insulators is discussed in Section 3.2.
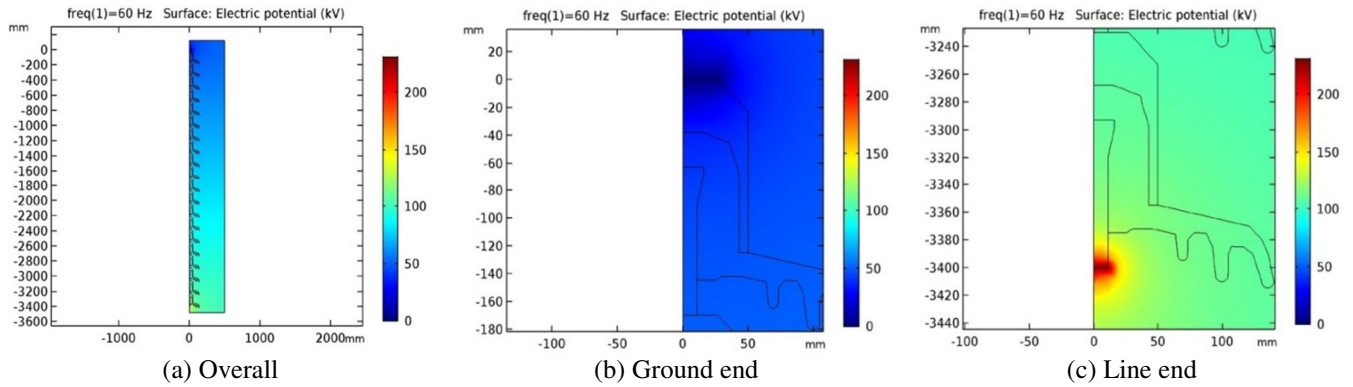

(a) Overall   (b) Ground end   (c) Line end

Fig. 8 Potential distribution of glass insulators for different scenarios

(a) Overall   (b) Ground end   (c) Line end

Fig. 9 Electric field distribution of silicon insulators for different scenarios

(a) Overall   (b) Ground end   (c) Line end
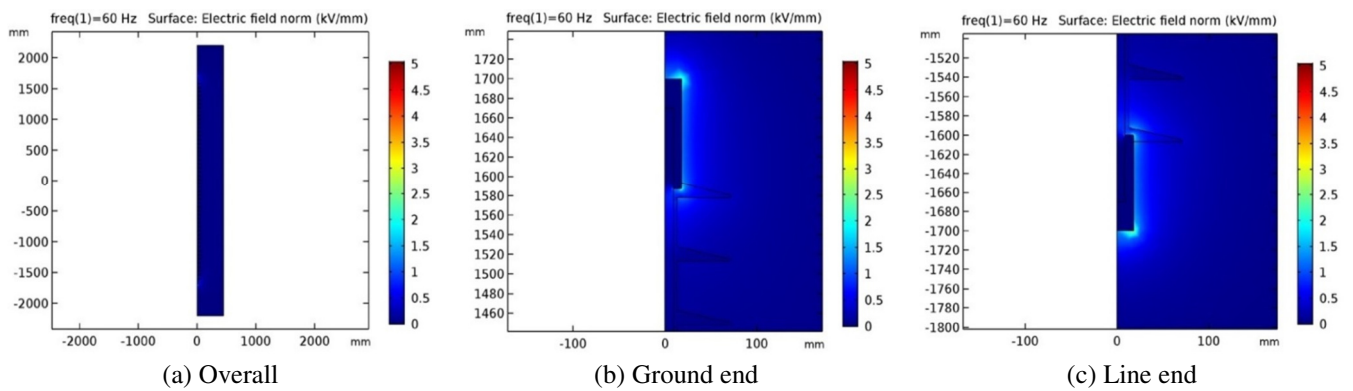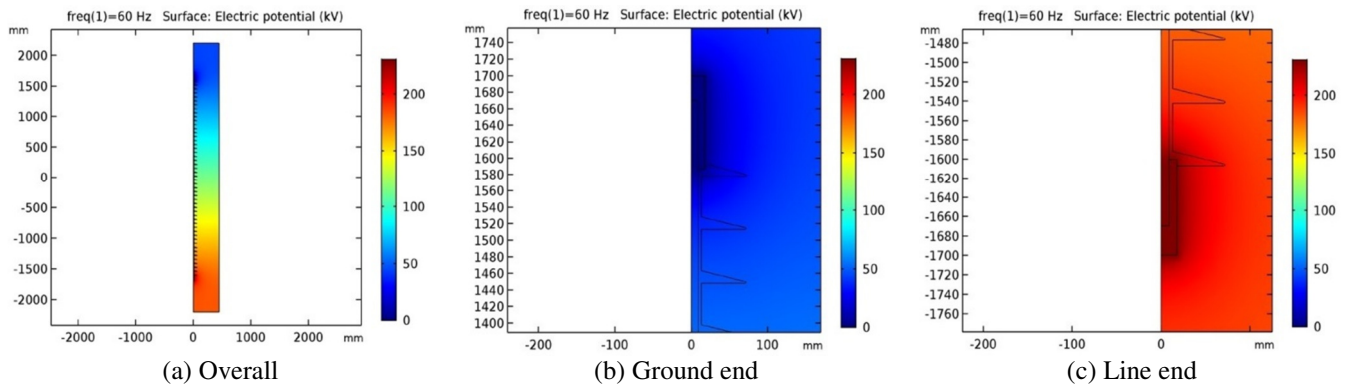
Fig. 10 Potential distribution of silicon insulators for different scenarios

(a) Electric field distribution   (b) Potential distribution

Fig. 11 3-D plot of glass insulators
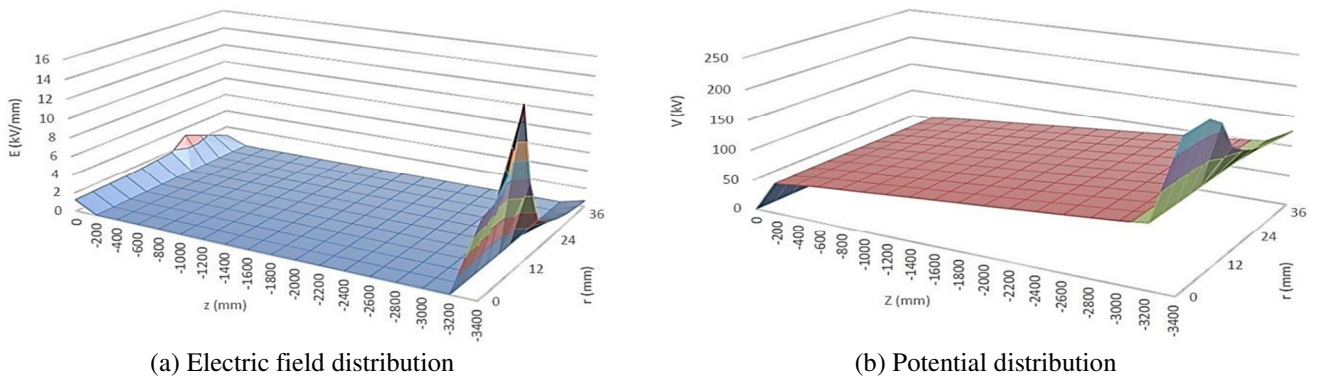
(a) Electric field distribution   (b) Potential distribution
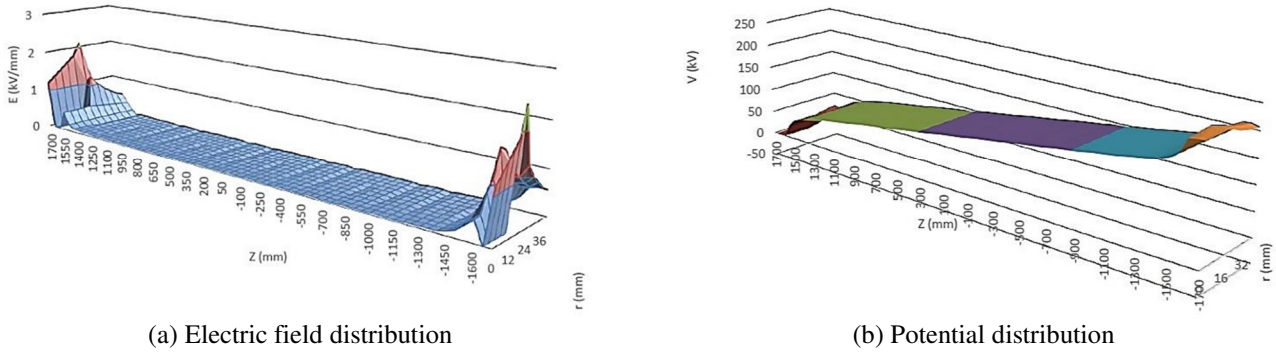
Fig. 12 3-D plot of silicon rubber insulators

3.2. Part 2

For optimization, different corona ring diameters have been considered and compared (from Table 1). [11]. COMSOL simulations have been performed for each ring specification and the corresponding obtained results are summarized in Table 5.

Table 5 Comparison of different corona rings

| Ring # | Dimension Characteristics | | Ring Position (h) | Maximum E (kV/mm) |
	Ring measurement (R)	Ring tube breadth (r)		
Without ring	-	-	-	3.03
Ring #1	32 inches (816 mm)	2.44 inches (62 mm)	-1650 mm	1.82
Ring #2	28 inches (711 mm)	2.44 inches (62 mm)	-1650 mm	1.73
Ring #3	24 inches (610 mm)	2.44 inches (62 mm)	-1650 mm	1.96
Ring #4	20 inches (508 mm)	2.44 inches (62 mm)	-1650 mm	1.79
Ring #5	16 inches (406 mm)	2.44 inches (62 mm)	-1650 mm	1.77
Ring #6	12 inches (305 mm)	2.44 inches (62 mm)	-1650 mm	1.81
Ring #7	8 inches (203 mm)	2.44 inches (62 mm)	-1650 mm	2.37
Ring #8	6 inches (152 mm)	2.44 inches (62 mm)	-1650 mm	1.81
Ring #9	32 inches (816 mm)	3.44 inches (87 mm)	-1650 mm	1.77
Ring #10	28 inches (711 mm)	3.44 inches (87 mm)	-1650 mm	1.79
Ring #11	24 inches (610 mm)	3.44 inches (87 mm)	-1650 mm	3.00
Ring #12	20 inches (508 mm)	3.44 inches (87 mm)	-1650 mm	2.42
Ring #13	16 inches (406 mm)	3.44 inches (87 mm)	-1650 mm	1.77
Ring #14	12 inches (305 mm)	3.44 inches (87 mm)	-1650 mm	1.79
Ring #15	8 inches (203 mm)	3.44 inches (87 mm)	-1650 mm	1.67
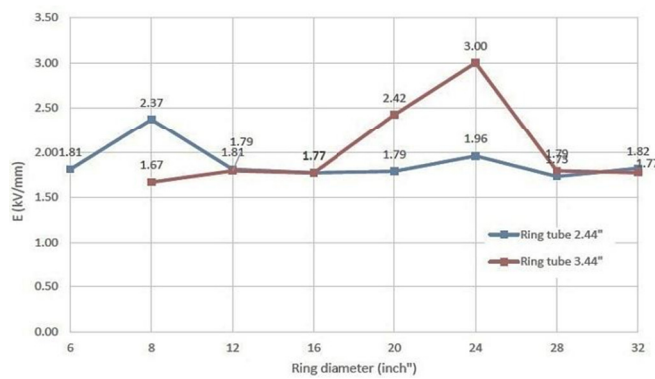
Fig. 13 Corona ring results of electric field distribution

Fig. 13 illustrates the electric field distribution results. The following points may be noted from the results:

(1) The electric field (1.67 kV/mm) is minimum in the case of Ring #15 where the ring diameter is 8 inches and the ring tube is 3.44 inches.

(2) Of the 15 rings simulated, 3 rings are observed to be still above the corona inception threshold: Ring #7, Ring #11, and Ring #12.

4. Conclusions

In this study, the electric field distribution and potential distribution over two suspension-type insulators (glass and NCI (silicon rubber)) connecting to 400 kV transmission systems were studied. The most commonly used silicon rubber insulators are prone to corona damages and they are generally used along with suitable corona rings with appropriate specifications to ensure voltages above 230 kV. It is recommended that these simulations be accompanied by laboratory tests on various corona rings to confirm the simulations results. The outcomes were empowered for also investigation toward thusly.

From Table 6, it can be seen that the estimations of the maximum electric field stress acquired by optimizing the corona ring are within the corona inception threshold value and are indeed very low when compared with the values obtained for the insulators without corona rings. From the results, it can be observed that the potential distribution along the insulator can be increased and the electrical stress can be minimized by adding a corona ring. It can be concluded that the corona ring can enhance the lifetime of an insulator.

In future studies, the effect of air temperature, humidity, and icing on the corona-related phenomena of the standard silicon rubber insulators with corona rings should be investigated.

Table 6 Summary of corona ring optimization for silicon rubber insulator

Ring #	Ring measurement (R)	Ring tube breadth (r)	Maximum E (kV/mm)	Description
Without ring	-	-	3.03	Above corona inception threshold
Ring #15	8 inches (203 mm)	3.44 inches (87 mm)	1.67	Minimum E

Conflicts of Interest

The authors declare no conflict of interest.

References

[1] R. A. Bernstorf, "Insulators 101 Design Criteria," IEEE PES T&D 2010, April 2010, pp. 1-5.

[2] S. Ilhan, A. Ozdemir, and H. Ismailoglu, "Impacts of Corona Rings on the Insulation Performance of Composite Polymer Insulator Strings," IEEE Transactions on Dielectrics and Electrical Insulation, vol. 22, no. 3, pp. 1605-1612, June 2015.

[3] P. Alotto and L. Codecasa, "Corona Discharge Simulation of Multi Conductor Electrostatic Precipitators," IEEE Transactions on Magnetics, vol. 52, no. 3, pp. 1-4, March 2016.

[4] P. Wang, Y. Zhao, F. Lv, K. Li, and Y. Ding, "Distribution of Electric Field and Structure Optimisation on the Surface of A ±1100 kV Smoothing Reactor," IET Science, Measurement & Technology, vol. 13, no. 3, pp. 441-446, May 2019.

[5] X. Zhao, X. Yang, J. Hu, H. Wang, H. Yang, Q. Li, et al., "Grading of Electric Field Distribution of AC Polymeric Outdoor Insulators Using Field Grading Material," IEEE Transactions on Dielectrics and Electrical Insulation, vol. 26, no. 4, pp. 1253-1260, August 2019.

[6] R. Lings, EPRI AC Transmission Line Reference Book—200 kV and Above, 3rd ed. CA: Palo Alto, 2005

[7] R. Anbarasan and S. Usa, "Electrical Field Computation of Polymeric Insulator Using Reduced Dimension Modeling," IEEE Transactions on Dielectrics and Electrical Insulation, vol. 22, no. 2, pp. 739-746, April 2015.

[8] F. Huo, P. Zhang, Y. Yu, Q. Liu, L. Chu, and X. Wang, "Electric Field Calculation and Grading Ring Design for 750 kV Four-Circuits Transmission Line on the Same Tower with Six Cross-Arms," The Journal of Engineering, vol. 2019, no. 16, pp. 3155-3159, March 2019.

[9] F. W. Peek Jr, Dielectric Phenomena in High Voltage Engineering, McGraw-Hill Press, New York, 1929.

[10] B. M'hamdi, M. Teguar, and A. Mekhaldi, "Optimal Design of Corona Ring on HV Composite Insulator Using PSO Approach with Dynamic Population Size," IEEE Transactions on Dielectrics and Electrical Insulation, vol. 23, no. 2, pp. 1048-1057, April 2016.

[11] Hubbell Power Systems Inc., "Recommended Corona Ring Installation Table", November 10, 2019 http://www.hubbellpowersystems.com/insulators/trans/suspension/quadrisil/corona.asp.

[12] S. Ilhan and A. Ozdemir, "380 kV Corona Ring Optimization for AC Voltages," IEEE Transactions on Dielectrics and Electrical Insulation, vol. 18, no. 2, pp. 408-417, April 2011.

[13] E. Brasca, E. Comellini, and D. Dell'Olio, "Power Arc on Insulator Strings: Testing Procedures and Design of Guard Devices for HV Transmission Lines," IEEE Transactions on Power Apparatus and Systems, vol. PAS-89, no. 3, pp. 420-428, March 1970.

[14] T. Doshi, R. S. Gorur, and J. Hunt, "Electric Field Computation of Composite Line Insulators Up to 1200 kV AC," IEEE Transactions on Dielectrics and Electrical Insulation, vol. 18, no. 3, pp. 861-867, June 2011.

[15] J. Wang, B. Yue, X. Deng, T. Liu, and Z. Peng, "Electric Field Evaluation and Optimization of Shielding Electrodes for High Voltage Apparatus in ±1100 kV Indoor DC Yard," IEEE Transactions on Dielectrics and Electrical Insulation, vol. 25, no. 1, pp. 321-329, February 2018.

[16] S. Heshmatian and A. Gholami, "Adjusting the Electric Field and Voltage Distribution along a 400 kV Transmission Line Composite Insulator Using Corona Ring," 2015 2nd International Conference on Knowledge-Based Engineering and Innovation (KBEI), November 2015, pp. 196-201.

[17] W. Sima, F. P. Espino-Cortes, E. A. Cherney, and S. H. Jayaram, "Optimization of corona ring design for long-rod insulators using FEM based computational analysis," Conference Record of the 2004 IEEE International Symposium on Electrical Insulation, October 2004, pp. 480-483.

[18] M. Farzaneh and W. A. Chisholm, Insulators for Icing and Polluted Environments, IEEE Press, Wiley, 2009.

[19] M. Bouhaouche, A. Mekhaldi, and M. Teguar, "Improvement of Electric Field Distribution by Integrating Composite Insulators in a 400 kV AC Double Circuit Line in Algeria," IEEE Transactions on Dielectrics and Electrical Insulation, vol. 24, no. 6, pp. 3549-3558, December 2017.

[20] M. Kanyakumari, R. S. Shivakumara Aradhya, H. Jangawala, and G. K. Xianghe, "Control of Electric Field and Voltage Distribution of a 765kV System Polymeric Insulator Used in Indian Transmission Systems," 2012 IEEE 10th International Conference on the Properties and Applications of Dielectric Materials, July 2012, pp. 1-4.

[21] C. Zachariades, S. M. Rowland, I. Cotton, V. Peesapati, and D. Chambers, "Development of Electric-Field Stress Control Devices for a 132 kV Insulating Cross-Arm Using Finite-Element Analysis," IEEE Transactions on Power Delivery, vol. 31, no. 5, pp. 2105-2113, October 2016.

[22] C. Guo, L. Liu, H. Yu, Y. Ma, H. Mei, and L. Wang, "Electric Field Distribution Calculation and Analysis of Composite Insulators Operating on Double Circuit Transposition Tower in 500kV Transmission Lines," 2019 2nd International Conference on Electrical Materials and Power Equipment (ICEMPE), April 2019, pp. 486-489.

[23] M. Bouhaouche, A. Mekhaldi, and M. Teguar, "Composite Insulators in a 400 kV AC Line in Algeria for Improving Electric Field Distribution," 2018 International Conference on Electrical Sciences and Technologies in Maghreb (CISTEM), October 2018, pp. 1-5.

[24] A. Hassanvand, H. A. Illias, H. Mokhlis, and A. H. A. Bakar, "Effects of Corona Ring Dimensions on the Electric Field Distribution on 132 kV Glass Insulator," 2014 IEEE 8th International Power Engineering and Optimization Conference (PEOCO2014), 2014, pp. 248-251.

[25] R. Kacprzyk and W. Bretuj, "Photoconduction in Outdoor Insulation Materials," IEEE Transactions on Dielectrics and Electrical Insulation, vol. 24, no. 2, pp. 1045-1050, April 2017.